Journal of Muscle Research and Cell Motility **20**: 517–527, 1999.

Development of muscle-specific features in cultured frog embryonic skeletal myocytes

GRIGORY A. NASLEDOV[1,*], IRENE E. KATINA[2], DMITRY A. TERENTYEV[1], NICOLAY V. TOMILIN[3] and VALERY I. LUKYANENKO[1]

[1]*Sechenov Institute of Evolutionary Physiology and Biochemistry, 44 Thorez av., 194223 St. Petersburg, Russia;* [2]*Department of Biophysics, St. Petersburg University, 199034 St. Petersburg, Russia;* [3]*Institute of Toxicology, 193019 St. Petersburg, Russia*

Received 1 December 1998; accepted in revised form 6 May 1999

Abstract

To study the development of muscle-specific features during myogenesis, we analysed the ultrastructure and voltage-dependent currents of frog embryonic skeletal myocytes maintained in culture for 10 days. The cells were maintained under culture conditions that prevented cell division, fusion and cell contacts with neuroblasts. The cell surface was estimated morphometrically and from cell capacity and the values obtained were used to calculate ion current densities. It was shown that the expression of all main types of voltage dependent ionic currents occurs during the first 3–5 days. Na^+ maximum specific conductance at days 1–2 was low but by day 7 it showed a 20-fold increase. The magnitude of Na^+ current densities increased 16-fold from day 1 (3.6 μA/cm) to the day 7 (58.1 μA/cm). The maximum specific K^+ conductance increased almost 3-fold during the first 5 days. In contrast to the other types of currents, I_K undergoes qualitative changes. Sodium action potentials, whose amplitude and time course depend on g_{Na}/g_K ratio, appeared from day 4 in culture, when myofibrils and the T-system also developed. The amplitude of DHP-sensitive slow I_{Ca} increased in parallel with the development of the T-membrane. $I_{Ca,S}$ density per unit of T-membrane area reached an equilibrium of ca., 17 μA/cm^2 on the day 4 and then remained stable until the end of the period of observation. These studies demonstrate that muscle-specific characteristics including morphology and excitatory properties begin to develop on the third day and resemble those of adult muscle cells by the sixth day in culture.

Introduction

It is known that single cultured skeletal myocytes are able to express a number of muscle-specific properties and maintain differentiated morphology. The cells express contractile proteins and develop sarcomeres (Okazaki and Holster, 1966; Stainberg *et al.*, 1971; DeCino and Kidokoro, 1985; Kidokoro and Saito, 1988), and the contacts between T-tubules and SR, which are responsible for excitation-contraction coupling (ECC) (Constantin *et al.*, 1995), are established. Cultured myo- cytes also develop voltage-dependent ion channels, which provide electrical excitability of the cells (Frelin *et al.*, 1981; DeCino and Kidokoro, 1985; Gilbert and Moody-Corbett, 1989; Zemkova *et al.*, 1989; Lukyanenko *et al.*, 1993). In most of these studies the data were obtained in culture systems selected at specific developmental stages and from different animal species, and their interpretation was complicated by the fact that the cells underwent fusion. So far, the coordination of changes in the contractile and tubular structures, and in the membrane excitability during development, has not been studied continuously stage by stage.

The present study was undertaken to determine the sequence of events in the development of muscle-specific morphological structures and electrophysiological processes in cultured embryonic frog skeletal muscle cells. The culture conditions selected prevented both the division and fusion of myocytes into myotubes. We have specifically investigated: (1) the progressive changes in voltage-dependent ion currents required in cell excitability, (2) the development of contractile filaments and T- and sarcotubular systems, responsible for ECC, and (3) the relationship between this morphological development and the changes in ion currents and cell excitability.

Materials and methods

Cell culturing

Myocyte cultures were prepared from early neurula embryos of *Rana temporaria*, as previously described (Lukyanenko *et al.*, 1993). The dorsal portions of the embryos were dissected in 60% Medium 199 M (Institute of Polyomyelitis, Academy of Medical Sciences of

* To whom correspondence should be addressed: Fax: 7(812) 552-3012; E-mail: nasledov@nasl.ief.spb.su

Russia) with 2% foetal calf serum (Sigma), and 50 U/ml penicillin and 50 μg/ml streptomycin (Russia), then washed for 10 min in calcium and magnesium-free solution containing 50.4 mmol/l NaCl, 0.67 mmol/l KCl, 0.86 mmol/l KH_2PO_4, 16 mmol/l Na_2HPO_4, 2.4 mmol/l $NaHCO_3$ and 1.9 mmol/l EDTA. During the dissociation into single cells the ectoderm was stripped and removed, and mesodermal and neural cells were transferred onto cover slips in 40 mm Petri dishes. The growth medium contained 55% Medium 199 M, 10% foetal calf serum, 50 U/ml penicillin and 50 μg/ml streptomycin.

In order to arrest cell fusion, some authors (Easton and Reich, 1972; Paterson and Strohman, 1972) used a low Ca^{2+} concentration. However, we used culture medium with a normal Ca^{2+} concentration, which is known to be important in cell homeostasis. We prevented the fusion of myocytes by plating the cells under the sparse conditions, about 200 myocytes per 40 mm Petri dish, and by increasing the serum concentration. In addition, we used Medium 199 M containing a low concentration of folic acid which is required for the synthesis of thymidylic acid preventing cell divisions (Teylor-Papadimitrou and Rozengurt, 1979). The cells were studied after 1 to 10 days in culture. The selected myocytes did not show any contacts with neuroblasts or with each other.

Patch-clamp recording and data analysis

The conventional whole-cell patch-clamp was used to record voltage-clamp membrane currents and current-clamp membrane potential. The circuit was similar to that described by Hamill *et al.* (1981), with a 0.5–10 GΩ head-stage feedback resistor. The amplifier List (EPC-7, Medical systems) was used. The resistance of patch electrodes filled with standard solution ranged between 3 and 5 MΩ. The seal resistance was 5–30 GΩ and the input resistance of cells was 1–5 GΩ. Experiments were started 10–15 min after the whole-cell configuration was established. The membrane potential was held at −80 or −90 mV. Data acquisition and analysis were performed by IBM-compatible 486 computer with original software.

Experiments were performed at room temperature (18–20°C). Mean ± standard errors of mean (SEM) are given.

Solutions and chemicals

The basic external solution (Ringer) contained 120 mmol/l NaCl, 1.5 mmol/l KCl, 2 mmol/l $CaCl_2$ and 8 mmol/l HEPES-NaOH (Sigma), pH 7.4. The pipettes were filled with a solution containing 110 mmol/l KCl, 1 mmol/l $CaCl_2$, 1 mmol/l $MgCl_2$, 10 mmol/l K_2EGTA (Sigma), 8 mmol/l HEPES-KOH (Sigma), pH 7.2. To study inward ion currents, KCl in the solution was replaced by 60 mmol/l CsCl and 50 mmol/l TEA-Cl. When necessary, tetrodotoxin (Sankyo), 4-aminopyridine (Sigma) and nifedipine (Sigma) were added into the Ringer solution.

Microscopy

For ultrastructural analysis, attached cells were fixed for 1 h in 2.5% glutaraldehyde buffered with 100 mmol/l Na-cacodylate buffer at pH 7.2. These operations were performed at room temperature. The samples were washed in 100 mmol/l solution of Na-cacodylate buffer with 0.034 g/ml sucrose and post-fixed in 1% osmium tetroxide with the same buffer at 4°C for 1 h. To mark the surface membrane and the internal membranes connected with the external environment, Ruthenium Red (RR)–$[Ru_3O_2(NH_3)_{14}]^{6+}$ (Serva)–in combination with aldehyde and osmium fixatives was used (Frank *et al.*, 1977; Luft, 1966). The final RR concentration in fixture solutions was 0.05%. The samples were embedded in Araldite after dehydration through increasing concentrations of ethanol and acetone. After Araldite polymerization, the cover slips were separated from the block by immersion in liquid nitrogen for a short time. Ultrathin sections (up to 0.1 μm) were cut by LKB Ultratome V, mounted on carbon films and stained with lead citrate, or mounted on grids and stained with lead citrate and uranyl acetate.

The ultrathin sections were examined in a JEM-100B electron microscope at 80 kV. The surface area of the myocytes was determined by means of diffraction lattice replica. The surface of structures labelled with RR was determined using high magnification and then calculated with respect to the volume unit, considering differences in magnification. The square grid with 4.1 mm step was used in morphometrical experiments. The test system was put on photoplates under Sitte angles of −19° or 71° to the myocyte long axis which are optimal for anisotropic structures (Eisenberg *et al.*, 1974). The cover slips (24 mm × 24 mm) with fixed cells (in 96% ethanol) were examined by means of a light microscope. The number of spindle-shaped cells was counted, and length and width were measured.

Results

Cell morphology

After plating the mononuclear myocytes became spindle-shaped and, under the sparse conditions used in these experiments, did not contact each other (Figure 1). During the whole period of culturing, the cell width remained steady ranging between 12 and 14 μm, while the cell length increased from ca. 80 μm in the first 24 h to 250 μm by day 10 (Table 1).

During the 1–2 days of plating the cells had round nuclei, which occupy the central part of the cell. At this developmental stage short filament bundles, apparently myosin filaments, 10–15 nm in diameter and ca. 1 μm long, were also observed. They were localized primarily

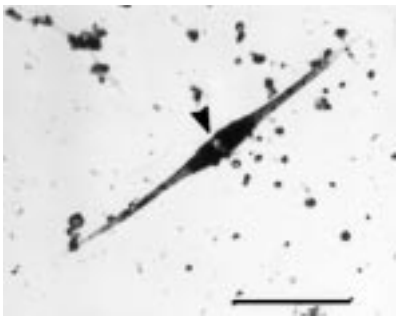

Fig. 1. The frog skeletal myocyte at the third day after plating. The single nucleus is indicated by an arrowhead. Bar = 70 μm.

to the peripheral cytoplasm just beneath the cell membrane (Figure 2a). RR formed a thin electron-dense layer on the cell surface. The membranes of vesicles or short tubes, near the cell surface, were also stained by RR. The groups of such vesicles and tubes could also form small chains just beneath the cell surface, which were oriented longitudinally to the cell axis (Figure 2b). In several cases the contact of these tubular structures with extracellular space was observed.

Muscle-specific structures began to develop on the third day in culture and extensive development of the contractile apparatus and of the internal tubular system was observed. At this time numerous myofilaments began to appear, predominantly near the cell surface. Many of them were already organized into sarcomeres and directed along the cell axis (Figure 3a). Large liposomes and numerous small round lizosomes continued to occupy the central part of the cell, as well as the nucleus (Figure 3a). A thin layer of RR was visible on the internal surface of T-tubules. The tubules were partially filled with electron-dense material (Figure 3b).

Intensive development of myofibrils and sarcomeres continued until 6–7 days in culture. At this time the myofibrils with well differentiated sarcomeres and regularly arranged triads occupied a considerable area of the cytoplasm, with sarcomere details, including Z-lines, H-zones and M-bands, clearly visible. The length of the sarcomere was about 1 μm. The triads were regularly arranged near Z-lines in all sarcomeres. T-tubules in

Table 1. Age-dependent changes in myocyte size, capacitance and specific area of T-system

	Age, day									
	1	2	3	4	5	6	7	8	9	10
R, μm ($n > 40$)	6.23 ± 0.08	6.15 ± 0.09	5.71 ± 0.08	6.42 ± 0.07	6.50 ± 0.07	6.78 ± 0.07	6.80 ± 0.07	6.80 ± 0.08	7.05 ± 0.09	7.00 ± 0.09
l, μm ($n > 40$)	79 ± 5	124 ± 5	148 ± 5	170 ± 7	185 ± 7	202 ± 8	215 ± 7	224 ± 6	231 ± 6	235 ± 8
S_s (10^{-6} cm^2)	13.6	21.4	24.5	29.5	32.1	34.7	37.3	39.03	39.9	40.8
C_m (pF)	13.8 ± 1.6 $n = 6$	21.6 ± 1.5 $n = 8$	26.2 ± 1.6 $n = 8$	34.5 ± 0.9 $n = 7$	37.9 ± 0.8 $n = 5$	43.4 ± 2.6 $n = 6$	50.1 ± 3.9 $n = 8$	52.8 ± 3.6 $n = 12$	53.7 ± 5.5 $n = 5$	56.0 ± 4.9 $n = 6$
ΔS (10^{-6} cm^2)	0.2	0.2	1.7	5.0	5.8	8.7	12.8	13.8	13.7	15.25
$\Delta S/S_s$	0.015	0.01	0.07	0.17	0.18	0.25	0.34	0.35	0.34	0.37
S_{in}/S_{ext}	0.07 ± 0.06	0.13 ± 0.08	0.25 ± 0.02	0.28 ± 0.06		0.28 ± 0.11		0.41 ± 0.13		0.45 ± 0.16

Radius (R), length (l) of cells and ratio of internal membranes area to surface area (S_{in}/S_{ext}) are the results of morphological studies. S_s, surface area calculated with Eq. 2; C_m, cell capacitance determined from capacitative transients; ΔS, difference between S_s and expected membrane area calculated from C_m (S_m) assuming a specific capacitance of 1 μF/cm^2; $\Delta S/S_s$, expected specific area of T-system. Values are mean ± SEM.

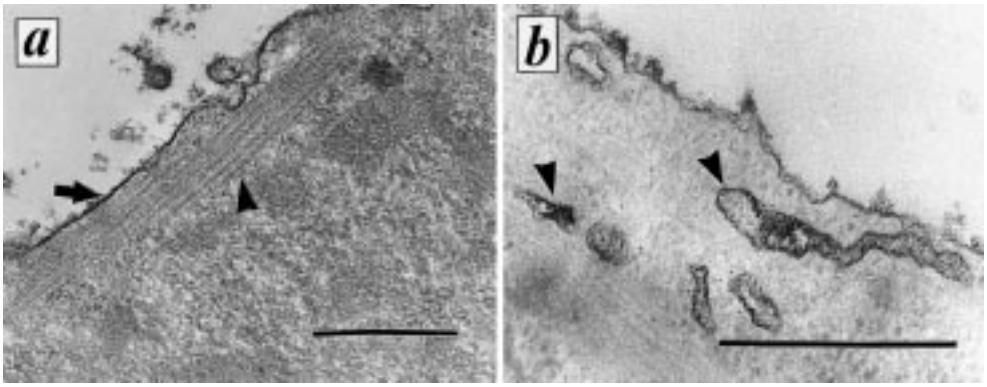

Fig. 2. Fragments of the myocyte at the first day of culturing. a. Rough-grained cytoplasm, and peripherally localized small bundles of myofilaments (arrowhead); the electron-dense layer of ruthenium red (RR) on the outer cell membrane (arrow). Bar = 500 nm. b. Vesicles and longitudinally directed membrane structures with the internal surface marked with RR (arrowheads), localized in the vicinity of the cell surface. Bar = 650 nm.

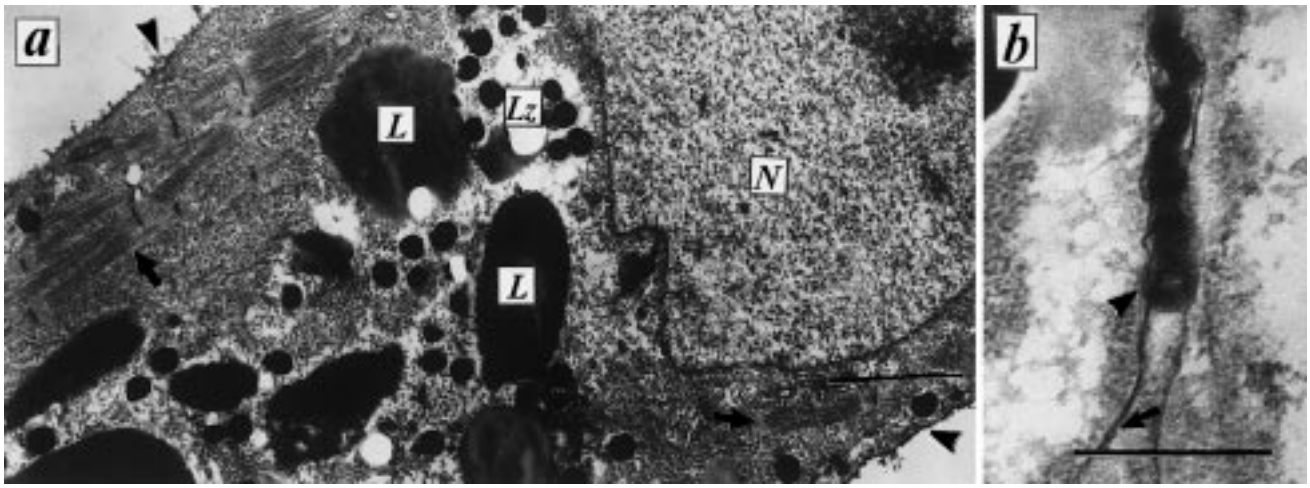

Fig. 3. Fragments of the myocyte at day 3 of culturing. a. The middle part of the cell with nucleus (N), large liposomes (L) and small dense lizosomes (Lz); peripherally localized myofilaments are constructing into myofibrils (arrows). Both edges of the cell are shown by arrowheads. Bar = 2 μm. b. Extended tubular structure with the internal surface of the membrane marked by RR (arrow), which is partially filled by the electron-dense content (arrowhead). Bar = 650 nm.

triads were labelled with RR (Figure 4a). These T-tubules were found to run transversely to the cell axis along the Z-lines (Figure 4b). In general, the structure of the contractile apparatus and triads at this stage of development looked very similar to that of adult frog muscle fibres.

From the 6–8 days in culture, myocytes exhibited the internal structure resembling that of differential muscle fibres. During the following period of culturing, dramatic changes in contractile filaments arrangement were observed: the cell cytoplasm became filled with disorganized bundles of myofilaments lacking longitudinal orientation and regular sarcomere organization. Triads were no longer visible in the normal positions (Figure 4c).

Morphometrical estimations of surface and T-tubule membranes

The cell surface (S_S) of the myocytes was estimated as the surface area represented by two circular cones. Taking into account the 4/3 flatting of the cross section (its elliptic shape), and that the length of the cell much exceeds its width, S_S can be estimated with the formula:

$$S_S = \pi l(R + 3/4R)/2 \quad (1)$$

where R is the radius of the cross section through the middle part of the cell, and l the cell length.

The values of myocytes S_S, estimated with equation [1] for different days in culture, are presented in Table 1. These values were used to calculate the membrane current densities and specific ionic conductances. In terms of these parameters it is possible to compare our data with those obtained elsewhere for adult frog skeletal fibres.

In order to estimate the extent of development of the T-system on different stages of culturing, morphometry of all membranes labelled by RR was performed on the electron micrographs. Intracellular membranes, labelled by RR and having contact with the external medium, were identified as T-tubule membranes. Consequently, the ratio of the volume density of intracellular labelled membranes to the external ones (S_{in}/S_{ext}) reflects the extent of T-system development (Table 1).

Age-dependent changes in the cell capacitance

The whole membrane area of the cell (S_m) can also be calculated from cell capacitance (C_m) assuming the specific capacitance as 1 μF/cm^2 (Marty and Neher, 1983). It is known that C_m, determined by capacitative current transients, reflects the capacitance of both external cell and the T-system membranes (Ribera and Spitzer, 1991). The differences between S_m and S_S for different days of culturing are presented in Table 1 (ΔS). $\Delta S/S_S$ in this Table reflects the expected specific area of T-system.

The values of cell surface area measured by the morphometrical and electrophysiological methods for 1–3-day old myocytes were similar and, consequently, very small values of $\Delta S/S_S$ were observed (0.015–0.07). After the 3rd day in culture, the membrane area values obtained by these two methods, begin to be different. This difference can be explained by the T-system appearance and development. $\Delta S/S_S$ rose from 0.17 (day 4) to 0.34 (day 7).

Evaluation of the specific T-system area, obtained by morphometric and electrophysiological methods (S_{in}/S_{ext} and $\Delta S/S_S$), showed a significant rise of T-membrane during culturing. Both methods gave similar results for myocytes on the final stages. However, the electrophysiological method, in contrast to the morphometric one, reveals the rise only after day 4 (Table 1).

Membrane currents and excitability

All main types of voltage-dependent ionic currents are expressed in myocytes developing in culture. The

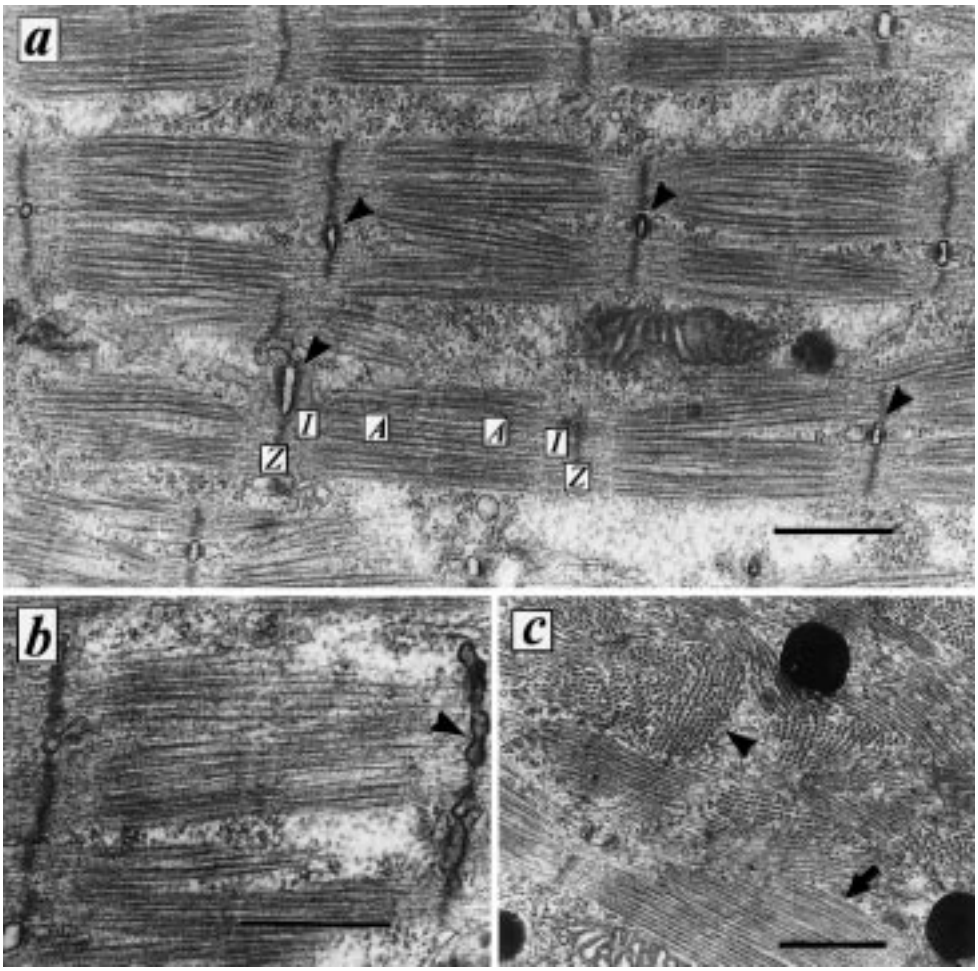

Fig. 4. Logitudinal sections of 3 parts from different myocytes at the late stages of culturing. a. Six days in culture: well-differentiated sarcomeres with their details: Z, Z-lines; A, anisotropic band; I, isotropic band; M, M-line; and the triads on the Z-line level (arrowheads). The length of sarcomeres is about 1.2 μm. b. Six days in culture: transverse T-system tubule stained by RR (arrowhead), running along the Z-line. c. Ten days in culture: sarcomere disorganization is obvious; longitudinally (arrow) and transversely (arrowhead) directed myofibrils are visible. All bars represent 500 nm.

dynamics and features of expression of each type are different. By day 5–6, all of them achieve magnitudes measurable in whole cell voltage-clamp experiments. The representative superimposed records of integral ion current in a 7-day old myocyte, elicited by depolarizing pulses to −20, −10, and 0 mV, are shown in Figure 5a. Fast inward sodium current (I_{Na}), delayed outward potassium current (I_K) and slow inward current through calcium channels (I_{Ca}) are obvious. Figures 5b and 5c illustrate the possibility of pharmacological separation of these components.

Na^+ and K^+ currents on early stages of culturing

During the first 2 days in culture, myocytes exhibit mainly the potassium component of integral ionic current (Figure 6, day 2). The time course of I_K at this stage is characterized by a relatively fast activation (time to peak 20–30 ms) and a slow inactivation rate. The non-inactivated part of I_K comprised 35–50% of the peak amplitude. During that period less than 15% of cells exhibited detectable fast inward current which can be identified as a TTX-sensitive voltage-dependent I_{Na}. The average maximal magnitude of I_{Na} was relatively small and did not exceed 200 pA.

Na^+ and K^+ currents after 3–7 days of culturing

At this stage of myogenesis, the integral ionic current included a component of inward I_{Na} with maximal amplitude, comparable with or exceeding the values of I_K (Figure 6, day 5). From day 1 to day 7 of culturing, the quantitative changes of I_{Na} are more markedly expressed (from 50 to 2200 pA) than those of I_K (from 500 to 1800 pA). The number of cells exhibiting tetrodotoxin-sensitive I_{Na} increased up to 80% by the day 7 in culture. The main characteristics of I_{Na} and I_K for different stages of culturing are shown on Figure 7 and Figure 8, respectively. The current densities were determined using morphometrical S_S (Figures 7c and 8d). The highest integral I_K density was observed on day 4 of culturing while the highest density for I_{Na} was observed much later (day 7 of culturing). During that period I_{Na} density rose 16-fold (from 3.6 to 58.1 μA/cm^2), and I_K density increased only 2-fold (from 26.7 to 51.9 μA/cm^2).

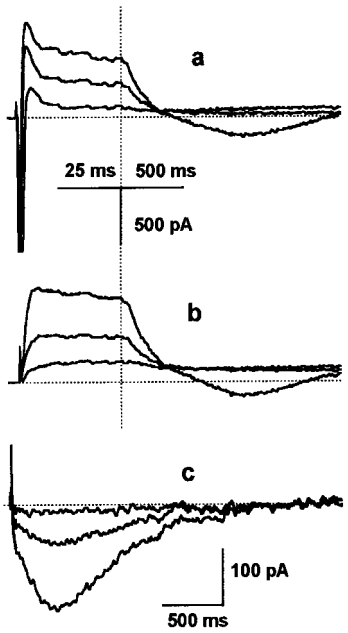

Fig. 5. Ion currents in myocyte on day 7 of culturing. Superimposed integral ion currents elicited by depolarizing pulses to −20, −10 and 0 mV from the holding potential −80 mV. a. Integral ion currents in standard extracellular solution. All types of ion currents are visually detectable in succession: fast inward I_{Na}, outward I_K, and slow inward I_{Ca}. b. Integral ion currents after addition of 1 μmol/l TTX. The fast inward I_{Na} component is abolished. Mention the non-linear scale of the time axes in a and b. c. Integral currents in the presence of TTX and 10 mmol/l 4-AP. Only the relatively slow component of inward current is seen, which is the sum of the fast and the slow Ca^{2+} currents.

During the entire period of culturing the main kinetic and pharmacological (TTX sensitivity) properties of I_{Na} remained unchanged and were similar to those of adult muscle fibre (Figure 7). Consequently, the dynamics in magnitude of I_{Na} amplitude and density reflect the increase in total number of Na channels per cell and its density during maturation. Kinetic properties of I_{Na} for all stages could be described in terms of the Hodgkin-Huxley model using the same set of equations and taking into account the differences in maximum specific sodium conductance (g_{Na}), which rose from 0.2 to 4.26 mS/cm^2 during 1–7 days of culturing.

Developmental changes in kinetics of K^+ currents

In contrast to I_{Na}, the kinetic properties of I_K changed considerably during myogenesis. The integral I_K became much more rapidly inactivated, although the activation rate did not change significantly within the same period (Figure 8). In addition, the non-inactivating part of I_K decreased from 35–50% on day 2 to 10–15% on day 7 of culturing. The time course of I_K decay was commonly complex and it was impossible to fit it with the monoexponential curve. To evaluate the inactivation rate, we used the time of decay to 50% of the peak amplitude ($t_{0.5}$). Developmental changes of $t_{0.5}$ are shown in Figure 8c. For the early stages $t_{0.5}$ at the test potential of 0 mV was more than 1 s, and until days 7–8 it decreased to 70–100 ms. Figure 8d shows that the peak potassium current density reached its maximum by day 4. However, the approximate values of maximum specific potassium conductance in terms of the Hodgkin-Huxley model (g_K), which were evaluated taking into account changes in the inactivation rate, exhibited the tendency to increase up to day 7 of culturing (1.2 mS/cm^2).

Developmental changes in Ca^{2+} currents

Inward I_{Ca} could be observed in most cells from day 4 of culturing, in the case of blocking I_K by using an intracellular solution containing Cs^+ and TEA^+ and/or

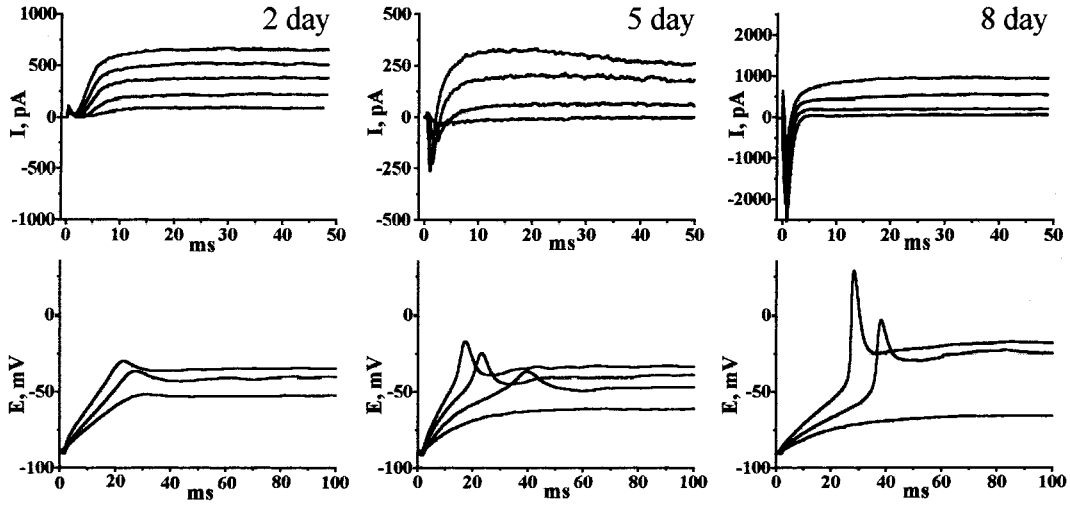

Fig. 6. Developmental changes of electrophysiological properties of cultured myocytes. Representative integral current and voltage records of the cells at 2, 5 and 8 days of development. Upper layer: superimposed current traces elicited in voltage-clamp mode by depolarizing pulses ranging between −30 and +10 mV in 10 mV increments. Holding potential −80 mV. Lower layer: changes of membrane potential elicited in current clamp mode by direct current stimulation. MP was shifted by injection of hyperpolarizing current to the level −90 mV. Day 2 myocyte: cell capacitance 25 pF, resting MP −32 mV, stimulating current densities 4, 6 and 8 pA/pF. Day 5 myocyte: capacitance 37 pF, resting MP −56 mV, stimulating current densities 2, 2.7, 4 and 5.4 pA/pF. Day 8 myocyte: capacitance 45 pF, resting MP −72 mV, stimulating current densities 2.2, 3.3 and 4.4 pA/pF.

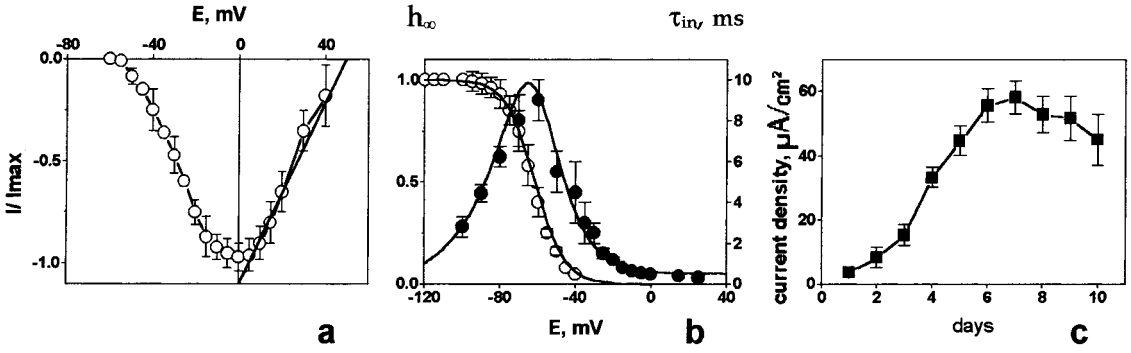

Fig. 7. Main kinetic characteristics of inward Na^+ current. a. Average peak current-voltage relation normalized to the maximum peak current value. b. Steady-state inactivation (h_∞, open symbols) and time constant of inactivation of I_{Na} (τ_{in}, filled symbols). Steady-state inactivation was achieved by 1 s voltage prepulses. The steady-state inactivation curve was fitted by a Boltzmann function: $h_\infty(V) = 1/\{1+\exp[(V-V_h)/k_h]\}$, with half-maximum inactivation voltage $V_h = -61.6$ mV, and a slope factor $k_h = 7.65$ mV. c. Na^+ current density against time of culturing. Data represent mean ± SEM; *n* for each data point ≥10.

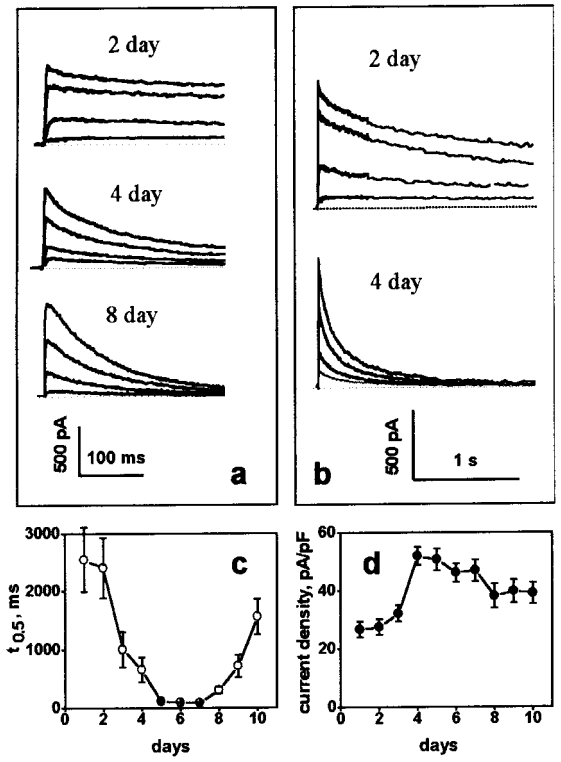

Fig. 8. Age-dependent changes in outward integral K^+ currents. a. Representative outward I_K recorded from myocytes of days 2, 4 and 8 of culturing, illustrating the difference in the rate of inactivation process. The membrane potential was changed from a HP of −80 mV to −30, −20, −10 and 0 mV. External solution contained 1 μmol/l TTX and 30 μmol/l nifedipine to abolish I_{Na} and L-type I_{Ca}. b. The same sets of superimposed traces for day 2 and day 4 in an extended time axis, showing the qualitative difference in inactivation process. c. Changes in the kinetics of inactivation of I_K in the course of culturing. Ordinate: time decay to the level of 0.5 ($t_{0.5}$) from the peak amplitude of I_K registered by potentials ±5 mV; abscissa: days in culture. d. I_K density against the time in culture. Data represent mean ± SEM; *n* for each data point ≥10.

the extracellular application of potassium channel blockers (Figure 5c). As a rule, the cells simultaneously exhibited two types of I_{Ca}, which can be distinguished by differences in kinetics, permeability and pharmacological properties (Figure 9). The first type was a well-known slow DHP-sensitive L-type I_{Ca} with high permeability to Ba^{2+} ions. The second type was a low-voltage activated DHP-insensitive fast I_{Ca}. Figure 9b shows current-voltage relations for $I_{Ca,f}$ and $I_{Ca,s}$. The maximum amplitude of both types of I_{Ca} increased during culturing and reached 300 pA by day 9–10.

During day 1 after plating the myocyte occurrence frequency with I_{Ca} of any type measurable in standard conditions was less than 15%, but with DHP agonist CGP-IOS (10–50 μmol/l) and/or a high concentration of Ba^{2+} (8–80 mmol/l), the presence of the slow I_{Ca} was detected in more than 50% of cells. The fast I_{Ca} was found in ca. 25% of the 2–3-day old myocytes. To reveal it, we used extracellular solution with a high concentration of permeable ions (Ca^{2+} or Ba^{2+}) in the presence of nifedipine to abolish L-type current. Also the fast I_{Ca} could be revealed by the typical slow-tail currents during repolarization. The approximate values of I_{Ca} amplitude for this stage of culturing were recalculated with coefficients derived for CGP-IOS and high concentrations of Ba^{2+} or Ca^{2+} from the experiments performed on more advanced stages (Lukyanenko *et al.*, 1993, 1994).

The fast and slow types of Ca^{2+} channels differed also in dynamics of expression. The maximum amplitude of the fast I_{Ca} increased especially from the day 1 to day 6 culture (6–7-fold) (Figure 9d). In contrast, the maximal amplitude of the slow I_{Ca} increased with some delay after day 3 in a more marked way (ca. 20-fold), continuing uniformly from the very beginning to the end of cell culturing.

Ion currents on days 8–10 of culturing

During the last stages the electrophysiological quantitative indices demonstrated almost unchanged tendencies. We did not reveal significant differences in kinetic characteristics of I_{Na}, slow and fast I_{Ca} between day 7 and day 10 in culture, only the maximal amplitude of slow I_{Ca} continued to increase. The distinction is the recurring slowing of I_K inactivation (Figure 8c), with the contribution of non-inactivating component remaining negligible.

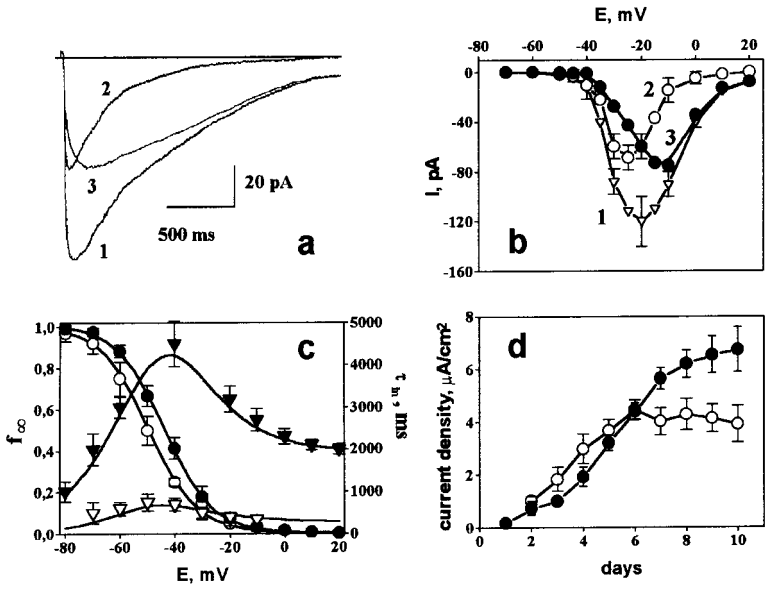

Fig. 9. Slow and fast types of Ca^{2+} currents. a. Integral ion currents elicited by depolarizing pulse to −20 mV from holding potential of −80 mV recorded before (curve 1) and after (curve 2) administration of 30 μmol/l of nifedipine. Internal solution contained 60 mmol/l Cs^+ and 60 mmol/l TEA^+ to abolish outward I_K, the external standard solution contained 1 μmol/l TTX to abolish I_{Na}. Curve 3 is the mathematical difference between curves 1 and 2, representing the DHP-sensitive I_{Ca}. b. Current-voltage relations for currents before (1, open circles) and after (2, filled circles) administration of nifedipine, and the difference between them (3, triangles). Data obtained from the same experiment as a. Bars indicate SEM of 2–4 recordings performed in the different moments after the beginning of experiment. The existence of deviations reflects rundown for I_{Ca}. c. Inactivation of slow and fast I_{Ca}. Steady-state inactivation curves (f_∞, circles) and time constants of inactivation (τ_{in}, triangles) of slow I_{Ca} (filled symbols) and fast I_{Ca} (open symbols). Steady-state inactivation was achieved by 30 s voltage prepulses; HP −80 mV. The data points were fitted by a Boltzmann function with half-maximum inactivation voltage V_h = −49.7 mV, and a slope factor k_h = 8.9 mV for fast I_{Ca} and V_h = −43.9 mV and k_h = 8.7 mV for slow I_{Ca}. d. Slow (filled circles) and fast (open circles) I_{Ca} densities against the time of culturing. Data represent mean ± SEM; *n* for each data point ≥10.

Membrane potential

Resulting membrane potential (RMP) was evaluated using the current-clamp mode of the whole-cell patch clamp. The mean values of RMP were very low for 1–3-day old myocytes (ca.−22 mV), and gradually increased from day 3 to day 8 of culturing (up to −57 to −60 mV) (Table 2).

Figure 6 shows typical changes of membrane potential (MP) in response to depolarizing pulses under the current clamp conditions. Only passive electrotonic responses or relatively slow changes of MP with the peak values less than −30 mV were recorded for the 1–3-day old myocytes. Starting from day 4 in culture, about 30% of cells generated responses, which can be identified as a typical sodium action potential (AP). Threshold, amplitude and time course of the AP depended preferentially on g_{Na}/g_K ratio (Figure 6, 5- and 8-day old myocytes; Table 2). This type of response can be abolished by TTX application and could not be changed by DHP blockers or activators of I_{Ca}.

Discussion

Repolarizing currents

Potassium channels are the most ubiquitous and diverse superfamily of membrane ion channels (Breitweiser, 1996; Rudy, 1988). We have determined that the outward I_K is the only component of the integral ion current present in the cells examined throughout the whole period of culture studied. Previously, in frog myocytes we have described 9 components of I_K that were based on differences in kinetics of activation (Lukyanenko *et al.*, 1993). In accordance with our data,

Table 2. Developmental changes of resting membrane potential, presence of action potentials and sodium/potassium maximum specific conductances ratio

	Age, day									
	1	2	3	4	5	6	7	8	9	10
RMP (mV)	−21.2 ± 0.7 *n* = 11	−22.3 ± 1.1 *n* = 9	−28.6 ± 3.5 *n* = 12	−34.2 ± 3.6 *n* = 14	−40.0 ± 3.5 *n* = 11	−45.0 ± 4.3 *n* = 14	−52.3 ± 5.8 *n* = 10	−57.0 ± 4.0 *n* = 14	−56.5 ± 9.0 *n* = 7	−59.2 ± 3.5 *n* = 10
AP	–	–	–	+	+	+	+	+	+	+
g_{Na}/g_K	<.45	1.14	1.71	2.93	3.15	3.28	3.80	3.88	4.10	4.57

RMP, resting membrane potential, Values are mean ± SEM, g_{Na}/g_K, ratio between sodium and potassium maximum specific conductances.

the greatest variety of components of I_K occurred on day 3–4 when the most dramatic increase in the I_K density was due mainly to the fast group of I_K. However, its maximum value (51.9 $\mu A/cm^2$) is 35-fold less than I_K density for adult frog fibres in sartorius muscle (Adrian *et al*., 1970) and 3-fold less than that in lumbricalis muscle (Lynch, 1985).

The I_K in frog skeletal myocytes undergo qualitative changes, preferentially concerning the kinetics of inactivation of the fast phase. Components of this phase of I_K have identical pharmacological properties and qualitatively similar characteristics of activation (Lukyanenko *et al*., 1993, 1995). Most probably they are subtypes of one family. The observed period (10 days) seems to be too short for the withdrawal of potassium channels' molecular complexes from plasma membranes, and the qualitative changes probably result from post-translational modification of the channels belonging to one family (Emsberger and Spitzer, 1995; Breitwieser, 1996; Xu *et al*., 1996).

Excitatory currents

It was shown by DeCino and Kidokoro (1985), in *Xenopus* myocytes, that single Na^+ channel conductance and kinetics do not change substantially during the development of frog myocytes under culture conditions, and that the recorded increase in AP was due to an increase in Na^+ channel density. In our experiments, too, kinetic properties of tetrodotoxin-sensitive I_{Na} did not change during culturing and were similar to those described in adult frog muscle fibres (Adrian *et al*., 1970, Adrian and Peachey, 1973). Thus, it appears that I_{Na} in embryonic skeletal myocytes is provided by a homogeneous population of Na^+ channels identical to the channels of mature skeletal muscle fibres. In this case differences in current density and specific maximum conductance directly reflect differences in the membrane density of Na^+ channels between mature muscle fibres and developing myocytes. However, even on day 7, when the maximum I_{Na} density was reached, it was 30-fold less than that previously observed in adult frog fibres from sartorius muscle (Adrian *et al*., 1970; Adrian and Peachey, 1973) and 8-fold less than from lumbricalis muscle (Lynch, 1985). This difference could be partly explained by a lack of neuronal influence, which increases AP and Na^+ channel density (DeCino and Kidokoro, 1985) and by arrested myocytes fusion. The results obtained in chicken embryonic skeletal muscle cells by Frelin *et al*. (1981) demonstrated that the increase in Na^+ channel density occurred mostly after the cell fusion and correlated with the increase in RMP. In our experiments on non-fusing myocytes RMP and Na^+ channel density also changed in parallel during culturing.

The activity of calcium-selective channels in myocytes under normal culture conditions became detectable on day 3. At this time, two types of I_{Ca} were observed: the well known slow L-type DHP-sensitive I_{Ca}, and the low-threshold, more rapidly activating DHP-insensitive I_{Ca}. The differences between the slow and the fast I_{Ca} in myocytes (Figure 9) resemble the well known differences between L- and T-type Ca^{2+} currents (Tsien *et al*., 1987). However, the kinetic parameters of the fast type of I_{Ca} differed substantially from a typical T-type described in other systems, including developing *Xenopus* myocytes (Moody-Corbett *et al*., 1989), and in adult frog *Rana temporaria* skeletal fibres (Hencek *et al*., 1988). The density of fast I_{Ca} in the present study increased until day 5 and then maintained at a steady level of about 4 $\mu A/cm^2$. The density of slow I_{Ca} continued to rise (Figure 8d) and, during the final stages of culturing, was close to that in adult frog muscle fibres (Almers and Palade, 1981; Huerta and Stefani, 1986; Hencek *et al*., 1988). Therefore, the expression of slow Ca^{2+} channels occurred with some delay, and then it ran in parallel with the increase in the T-tubule membrane area.

Kano (1975) showed that calcium action potentials in developing chicken skeletal muscle cells appear earlier than the mechanism for generation of sodium APs. However, despite the high density of I_{Ca} in frog myocytes, we did not observed calcium APs and did not reveal a detectable contribution of both types of I_{Ca} in sodium AP.

Structural differentiation

The main developmental features observed in this investigation on frog skeletal myocytes were similar to those described earlier on other kinds of cultured myocytes undergoing myogenesis (Franzini-Armstrong, 1986; Kidokoro and Saito, 1988; Flucher, 1992). Some differences between the developmental features observed in the present study and those previously mentioned may be due to the differences in species or the conditions we used to prevent cell fusion.

The myofilaments, in the form of short and very thin bundles, were seen already on the first day of culturing, but only near the cell surface. The width of the filaments corresponds to the myosin filament width. It should be noted that even when these cells exhibited disorganized contractile filaments, they were able to contract in response to membrane depolarization (Nasledov *et al*., 1992).

The sarcomere zones were first distinguished on day 4, but Z-lines were still obscure. The differentiated myofibrils were observed on day 6, and the Z-lines and H-zones with the M-bands were clearly seen. It is known that the formation of the contractile filaments in myotubes during myogenesis *in vivo* begins from the peripheral part of the cell to further spread to the centre (Franzini-Armstrong, 1986). The same sequence was observed in our case. The first myofilament bundles appeared on the periphery, and only on the 6th day myofibrils with well-differentiated sarcomeres were seen in the center of the cell, mainly in the paranuclear area. The myofibrils in the 6-day old myocytes looked very similar to those of the mature fibres, they occupied a

large part of the cell, but were separated from each other by wide strips of cytoplasm. After 8–10 days, dramatic sarcomere disorganization was observed. The myofibrils were dispersed into filament bundles, which were no longer uniformly oriented.

We used RR to mark the membranes, which had contact with the extracellular environment (Frank *et al.*, 1977). During the first days of culturing the membrane structures were represented by the vesicles located under the cell outer membrane. Some of the vesicles were fused with each other, forming twisted tubes of different shape and length. The length of the tubes gradually increased. The ratio of the surface area of these membranes to the area of the external cell membrane is increasing with the ageing of culture. It appeared that on day 3, some parts of RR marked tubules were filled with electron-dense material. Later on such phenomenon was observed no longer.

Our data suggest that there are two critical periods in frog myocytes structural development in culture. One occurs on day 3 in culture and is characterized by aggregation of myofilaments into myofibril-like structures resembling the first stages of sarcomere organization. At this time restricted tubular structures also appear. This may be the point when the cell makes a cell-lineage decision to switch from an unspecialized multipotential cell to a specialized muscle cell. It may be suggested that the third day in culture represents the stage when myocytes fuse under normal conditions. The second critical point in this *in vitro* system appears on the sixth day, when significant muscle cell differentiation was observed. These data suggest that myocyte fusion is not required for differentiation of the internal membrane system providing ECC. However, it is possible that the differentiation process is altered in the absence of fusion.

The myofibril and sarcotubular system disorganization may indicate the gradual death of myocytes.

Interrelations between the development of excitability and structural differentiation

Recent experimental progress has led to a better understanding of the mechanisms that control myogenesis in the embryo. Along with the identification of regulatory genes that are involved in controlling specific transcriptional events (Ludolph and Konietzny, 1995), many of the advances are the result of determining the role and expression of ionic currents, fusion and neuronal contacts (Moody-Corbett and Vigro, 1991; Constantin *et al.*, 1995; Linsdell and Moody, 1995).

During the first 3 days in culture, the T-membrane area values measured by morphometric method were different from those estimated on the basis of cell capacitance measurement (Table 1). The ultrastructure analysis demonstrated that the tubules detected by RR were partially filled with electron-dense material as well as vesicles under the cell surface membrane, which can be referred to the developing T-tubules. After the third day in culture, the T-tubules became empty and the contribution of T-system to cell capacitance became detectable suggesting that the electron-dense substance had insulating properties, and the T-tubules containing it were inaccessible for electrical signal transmission. From the third day the slow I_{Ca} became measurable in normal conditions and thereafter correlates with the increase in T-tubule membrane area. The data presented on Figure 9d for the slow I_{Ca} recalculated per unit of T-membrane area demonstrate that the value of density reaches the level of 15–18 $\mu A/cm^2$ to the fourth day and its following changes are negligible. We suggest that the increase in the total number of slow Ca^{2+} channels/DHP receptors directly depends on the T-membrane area growth and that the channel density on the T-membranes remains constant from the very appearance of these membranes and during the whole period of myocytes development.

The third and fourth days in culture are a period of fast development of the contractile apparatus and triads, of a sharp rise in densities of all current types and the first time when sodium AP can be recorded. Possibly, this period corresponds to the time of cell fusion under suitable conditions. Analysing our data we conclude that excitability and structural development occur in a coordinated manner.

After day 8, when the disorganization of myofibril structure occurred, all main tendencies in dynamics of expression of voltage-dependent ionic currents of myocytes remained unchanged. The maximum amplitude of the slow I_{Ca} continued to increase along with the growth of T-membranes area. The only obvious distinction was the recurring slowing of I_K inactivation (Figure. 8). However, the contribution of non-inactivating component remains insignificant. It can be concluded that myocytes during the last stages in culture maintain high level of synthetic activity, but the coordination of parallel development of excitability and morphological structures of ECC is disturbed.

Acknowledgements

This work was supported by grants N 96-04-50608 and N 99-04-49953 from the Russian Foundation for Basic Research.

References

Adrian RH, Chandler WK and Hodgkin AL (1970) Voltage clamp experiments in striated muscle fibres. *J Physiol Lond* **208:** 607–644.

Adrian RH and Peachey LD (1973) Reconstructing of action potential of frog sartorius muscle. *J Physiol Lond* **235:** 103–131.

Almers W and Palade PT (1981) Slow calcium and potassium currents across frog muscle membrane, measurements with vaseline-gap technique. *J Physiol Lond* **312:** 159–176.

Breitwieser GE (1996) Mechanisms of K^+ channel regulation. *J Memb Biol* **152:** 1–11.

Constantin B, Cognard C and Raymond G (1995) Myoblast fusion is not a prerequisite for the appearance of calcium current, calcium

release, and contraction in rat skeletal muscle cells developing in culture. *Exp Cell Res* **217:** 497–505.

Decino P and Kidokoro Y (1985) Development and subsequent neural tube effects on the excitability of cultured *Xenopus* myocytes. *J Neurosci* **5:** 1471–1482.

Easton TG and Reich E (1972) Muscle differentiation in cell culture. *J Biol Chem* **247:** 6420–6431.

Eisenberg BR, Kuda AM and Peter JB (1974) Stereological analysis of mammalian skeletal muscle. I. Soleus muscle of adult guinea pig. *J Cell Biol* **60:** 732–754.

Ernsberger U and Spitzer NC (1995) Convertible modes of inactivation of potassium channels in *Xenopus* myocytes differentiating in vitro. *J Physiol* **484:** 313–329.

Flucher BE (1992) Structural analysis of muscle development: transverse tubules, sarcoplasmic reticulum and the triad. *Dev Biol* **154:** 245–260.

Frank JS, Langer GA, Nudd LM and Seraydarian K (1977) The myocardial cell surface, its histochemistry, and the effect of sialic acid and calcium removal on its structure and cellular ionic exchange. *Circul Res* **41:** 702–714.

Franzini-Armstrong C (1986) The sarcoplasmic reticulum and transverse tubules. In: Engel A and Banker B (eds). Myology. (pp. 125–153). McGraw-Hill, New York.

Frelin C, Lombet A, Vigne P, Romey G and Lazdunski M (1981) The appearance of voltage-sensitive Na^+ channels during in vitro differentiation of embryonic chick skeletal muscle cells. *J Biol Chem* **256:** 12355–12361.

Gilbert R and Moody-Corbett F (1989) Four outward potassium currents in *Xenopus* skeletal muscle cells in culture. *Can J Physiol Pharmacol* **67:** Axiii–Axiv.

Hamill OP, Marty A and Neher E (1981) Improved patch-clamp techniques for high-resolution current recording from cells and cell-free membrane patches. *Pflügers Arch* **391:** 85–100.

Hencek M, Zacharova D and Zachar J (1988) Fast calcium currents in cut skeletal muscle fibres of the frogs *Rana temporaria* and *Xenopus laevus*. *Gen Physiol Biophys* **7:** 651–656.

Huerta M and Stefani E (1986) Calcium action potentials and calcium currents in tonic muscle fibres of the frog (*Rana pipiens*). *J Physiol Lond* **372:** 293–301.

Kano M (1975) Development of excitability in embryonic chick skeletal muscle cells. *J Cell Physiol* **86:** 503–510.

Kidokoro Y and Saito M (1988) Early cross-striation formation in twitching *Xenopus* myocytes in culture. *Proc Natl Acad Sci USA* **85:** 1978–1982.

Linsdell P and Moody WJ (1995) Electrical activity and calcium influx regulate ion channel development in embryonic *Xenopus* skeletal muscle. *J Neurosci* **15:** 4507–4514.

Ludolph DC and Konieczny SF (1995) Transcription factor families: muscling in on the myogenic program. *FASEB J* **9:** 1595–1604.

Luft JH (1966) Fine structure of capillary and endocapillary layer as revealed by ruthenium red. *Fed Proc* **25:** 1773–1783.

Lukyanenko V, Katina IE and Nasledov GA (1994) Voltage dependent fast calcium current in cultured skeletal myocytes of the frog *Rana temporaria*. *Gen Physiol Biophys* **13:** 237–246.

Lukyanenko V, Katina IE, Nasledov GA and Lonsky AV (1993) Voltage dependent ionic currents in frog cultured myocytes. *Gen Physiol Biophys* **12:** 231–247.

Lukyanenko V, Katina IE, Nasledov GA and Terentyev DA (1995) Pharmacological analysis of voltage-dependent potassium currents in cultured skeletal myocytes of the frog *Rana temporaria*. *Gen Physiol Biophys* **14:** 525–534.

Lynch C (1985) Ionic conductances of frog short skeletal muscle fibres with slow delayed rectifier currents. *J Physiol Lond* **386:** 359–378.

Marty A and Neher E (1983) Tight-seal whole-cell recording. In: Sakmann B and Neher E (eds). Single Channel Recording (pp. 107–122). Plenum Press, New York.

Moody-Corbett F, Gilbert R, Acbarali H and Hall J (1989) Calcium current in embryonic *Xenopus* muscle cells in culture. *Can J Physiol Pharmacol* **67:** 1259–1264.

Moody-Corbett F and Virgo NS (1991) Exposure to nerve does not affect the appearance of calcium currents in embryonic muscle. *Neuroreport* **2:** 437–440.

Nasledov GA, Lukyanenko V, Katina IE and Lonsky AV (1992) Ionic requirements for the activation of contraction in embryonic frog myoblasts in culture. *Gen Physiol Biophys* **11:** 153–159.

Okazaki K and Holtzer H (1966) An analysis of myogenesis *in vitro* using fluorescein-labeled antimyosin. *J Histochem Cytochem* **13:** 726–739.

Paterson B and Strohman RC (1972) Myosin synthesis in cultures of differentiating chicken embryo skeletal muscle. *Dev Biol* **29:** 113–138.

Ribera AB and Spitzer NC (1991) Differentiation of delayed rectifier potassium current in embryonic amphibian myocytes. *Dev Biol* **144:** 119–128.

Rudy B (1988) Diversity and ubiquity of K channels. *Neuroscience* **25:** 729–749.

Shainberg A, Yagil G and Yaffe D (1971) Alterations of enzymatic activities during muscle differentiation in vitro. *Dev Biol* **25:** 1–29.

Teylor-Papadimitrou J and Rozengurt E (1979) The role of thymidine uptake in the control of cell proliferation. *Exp Cell Res* **119:** 393–396.

Tsien RW, Hess P, McCleskey EW and Rosenberg RL (1987) Calcium channels: mechanisms of selectivity, permeation, and block. *Annu Rev Biophys Biophys Chem* **16:** 265–290.

Xu H, Dixon JE, Barry DM, Trimmer JS, Merlie JP, McKinnon D and Nerbonne JM (1996) Developmental analysis reveals mismatches in the expression of K^+ channel currents in rat ventricular myocytes. *J Gen Physiol* **108:** 405–419.

Zemková H, Vyskočil F, Tolar M, Vlachová V and Uječ E (1989) Single K^+ currents during differentiation of embryonic muscle cells in vitro. *Biochim Biophys Acta* **986:** 146–150.